Quantitative Analysis Method of Immunochromatographic Strip Based on Reinforcement Learning

Songming Liu[1*], Shaojun Zeng[2]

[1]Department of Instrumental and Electrical Engineering, Xiamen University, Xiamen, Fujian, 361005, China

[2]Department of Instrumental and Electrical Engineering, Xiamen University, Xiamen, Fujian, 361005, China

[*]Corresponding author's e-mail: 18030103869@163.com

Abstract. Gold immunochromatographic assay (GICA) is a widely used immunological detection technology with high sensitivity and high efficiency as well as simple operation. Traditional GICA is mainly based on instrument for qualitative detection. In response to the above questions, this paper aims to develop an automated detection framework for immunochromatographic strips that can adaptively improve the detection performance of the gold immunochromatographic strip (GICS) system. As a research hotspot of machine learning (ML), reinforcement learning (RL) has made many progresses in the field of image segmentation. In this paper, the RL method is applied to the GICS system for the first time. The RL agent provides an adaptive segmentation model for the newly obtained GICS images by learning the state features of the preprocessed images. It is worth noting that our method does not require a large training data set and simultaneously can effectively reduce the grayscale-based image feature space. The experimental results show that the proposed method has a good segmentation effect, and provides a reliable solution for the quantitative analysis of the GICS system.

1. Introduction

Gold immunochromatographic strip (GICS) is a medical immunochromatography technique that utilizes the antigen-antibody specific reaction to determine the concentration of a target substance in test sample. In the past decade, GICS has been extensively studied and widely used in biomedical and related fields for the determination of analyte in specimens due to its fascinating advantages like convenient, time-saving and low cost [1, 2]. To enhance the performance of GICS, biochemical researchers have introduced various material selection methods [3]. Development of GICS instrumentation has also aroused great scholarly interests. A GICS biochemical reaction model has been designed to optimize detection performance [4]. Additionally, image-based GICS methods for quantitative detection have become a novel hotspot for their simplicity and ease of operation. The key design specification of image-based systems lies in image processing technology for accurately distinguishing test and control lines from acquired GICS images.

In recent years, many methods including the Otsu threshold segmentation approach, cellular neural network method have been proposed in order to achieve effective segmentation of control lines and test lines of GICS images [5]. However, segmentation of GICS images still remains a challenge. Firstly, the GICS images obtained always have a lot of noises as a result of the influence of temperature or humidity, which brings us difficulty in effectively distinguishing the control line test

line; Secondly, for samples in low concentration, traditional image processing method may bring up unsatisfactory segmentation effect because there is nearly no difference between the lines and the background.

There are three main aspects of our work. (1) A preprocessing part is added in order to reduce the framework based on reinforcement learning is put forward. (2) A GICS images automatic detection framework based on reinforcement learning is put forward. (3) Corresponding relationship between analyte concentration and characteristic parameter has been established to achieve quantitative detection.

The remainder of this paper is organized as follows. Section II introduces of gold immunochromatographic strips. Principles and applications of reinforcement learning algorithms are provided in section III. Section IV describes how we apply the reinforcement learning model to GICS image segmentation. Evaluation of the experimental results and the performance of the proposed model are presented in section V. In the last part, we draw a conclusion.

2. The Gold Immunochromatographic Strips

Gold immunochromatographic strips (GICS) labeled with colloidal gold nanoparticles are based on an immunochromatographic process that exploits the high specificity of antigen-antibody reactions. GICS is able to provide rapid determination of target analyte. As shown in Figure 1, GICS is mainly composed of several components including a sample pad, an absorbent pad, a conjugation pad and a nitrocellulose membrane which is used as a reaction carrier. When the strip is dropped into a specimen solution, the solution is subject to capillary action in the direction of the absorbent pad, and the mark is dissolved when passing through the bond pad coated with the nano-gold particle mark. At the same time, the analyte in the specimen reacts with the label to form a complex substance in red or purple on the membrane, which is caused by the accumulation of gold nanoparticles on the control and test line. In particular, the signal intensity of the test line is directly related to the concentration of the target analyte in the specimen. Therefore, the concentration of the target analyte can be quantitatively analyzed by the signal intensity of the test line after the reaction [6].

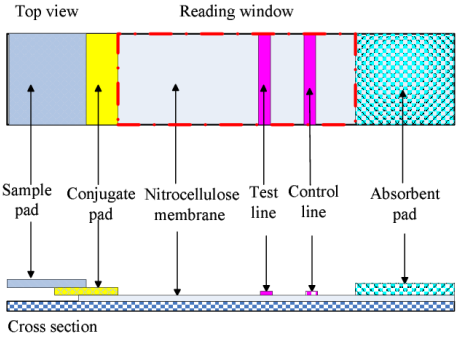

Figure 1. The schematic structure of the gold immunochromatographic strip.

In this paper, human chorionic gonadotropin (hCG) is used as the target analyte in the experiment. The quantitative detection of hCG concentration that can be used as a detection index for various gynecological diseases has positive and important significance. In this experiment, we select a variety of GICS strips with different hCG concentrations. Part of the images are shown in Figure 2. The main purpose of this paper is to set up a RL model to achieve precise segmentation and quantitatively analyze of GICS as well.

Figure 2. Images of GICS with different concentrations.

3. Reinforcement Learning

Reinforcement learning is an intelligent machine learning method that interacts with the environment. It enables the RL agent to self-adaptively determine the action taken in a particular state in order to maximize performance. The reinforcement learning system consists of several parts including state, action and reward [7, 8]. RL agent is a decision maker that constantly interacts with the environments and attempts to take action in specific states. Corresponding rewards will be obtained with the changing of state in the environment resulted from the action, which is fed back to the agent as generated experiences. As the learning experiences increased, the RL agent is capable to make the best decision for each state eventually to maximize its accumulated benefits. [9].

Q-Learning algorithm is one of the classic techniques proposed by Watkins that is used to learn the strategy for agent in model-free reinforcement learning system. In the Q-Learning algorithm, the value of the state-action pairs represents an estimate of the subsequent accumulated rewards when the RL agent takes action a at state s. The agent will adopt the action with the highest Q value in state s after the Q table has been learned. The Q-learning algorithm has a problem of how to choose action a in a given state s. The Boltzmann policy uses thermodynamic principles to decide how to choose the most appropriate one among many actions [10, 11]. In addition to Boltzmann policy there are other methods such as ε-greedy and greedy policy. The greedy policy selects the action with the highest immediate benefit each time according to the Q table while the ε-greedy policy selects the action with the highest Q value with probability ε or chooses any other action with the probability 1-ε. The Q-learning algorithms is presented in Figure 3.

Set values for learning rate α、discount rate γ、reward matrix R
Initialize $Q(s,a)$ to zeros
Repeat for each episode,do
  Select state s randomly
  Repeat for each step of episode,do
    Choose a from s using ε-greedy policy or Boltzmann policy
    Take action a obtain reward r from R, and next state s'
    Update $Q(s,a) \leftarrow Q(s,a) + \alpha[r + \gamma \max_{a'} Q(s',a') - Q(s,a)]$
    Set $s = s'$
    Until s is the terminal state
  End do
End do

Figure 3. Q-Learning algorithm.

4. Reinforcement Learning for the GICS images segmentation

Reinforcement learning has provided high-performance application in the field of image processing. In this paper, we provide a new method for segmentation of GICS images via RL. Figure 4 show the flowchart of GICS image segmentation based on reinforcement learning.

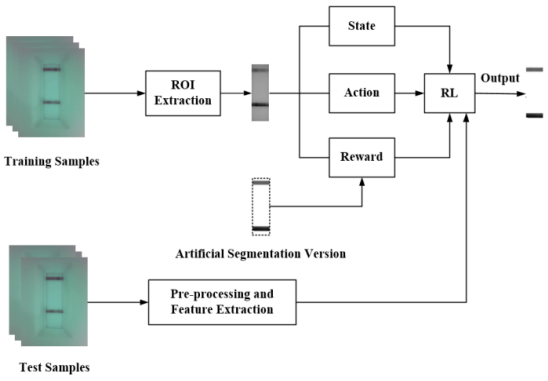

Figure 4. A general model for Reinforcement learning agent.

In our method, we first preprocess the initial acquired GICS images due to the inevitable noises from the manufacture and transmission process. After series of operations including filtering and denoising, we acquire the region of interest (ROI) shown in Figure 4. The ROI images have a common feature that the lines are darker while the other areas are brighter which can be regarded as two parts: the foreground (control line and test line) and the background (other areas). Based on it, we consider using clustering method to segment the ROI images from the aspect of pixel grayscales. We define a parameter to represent the grayscale of center point in foreground, and to stand for the grayscale of center point in background. Furthermore, we can determine which part a pixel belongs to by the following principles:

$$d_f = \sqrt{(p_i - p_f)^2} \tag{1}$$

$$d_b = \sqrt{(p_i - p_b)^2} \tag{2}$$

$$p_i = \begin{cases} 0 & d_f \le d_b \\ 255 & d_f > d_b \end{cases} \tag{3}$$

Where d_f describes the distance between p_i and p_f while d_b represents the distance between p_i and p_b. If d_f is smaller, then p_i is regarded in the foreground. Current segmentation result is acquired after all the pixels have been assigned. Besides, there is a manually identified best version of the segmentation for each image. The agent makes a comparison between them to evaluate the performance of current segmentation in the manner of giving it a reward value, and adjusts the values of p_f and p_b accordingly.

4.1. Defining the States

As the contents aforementioned, once the center point pair has been selected there is a segmentation result. We need to calculate the state value of that and in order to define the states, following two features have been considered: Regional features: In the GICS images, there are obvious differences between their background and foreground, where the performance of the segmentation could be told. Besides our segmentation result, we also employ a result from another effective approach such as OSTU. Then we make a comparison between the background and foreground of them to express a state factor. Edge feature: Under some circumstances, the discrimination between the background and foreground is not distinct sufficiently. Thus the edges play an important role in evaluating the performance of the segmentation. Similar to regional features, we make a comparison in terms of the edge features to serve as another state factor, where canny edge detection operator is utilized. Combining the two factors above, we obtain following formulas:

$$S_R = K_R \frac{\sum p_f \cap \sum p_b + \sum p_{f|OSTU} \cap \sum p_{b|OSTU}}{\sum p_f + \sum p_b} \tag{4}$$

$$S_E = K_E \frac{\sum p_{E|canny} \cap \sum p_{E|OSTU,canny}}{\sum p_{E|canny}} \tag{5}$$

Where S_R is regional features and S_E is edge features. K_R and K_E are both coefficients which determine the sparsity of the state space, p_f and p_b represent the pixel in the foreground and background, respectively. The same characteristics obtained from the OSTU method are denoted by $p_{f|OSTU}$ and $p_{b|OSTU}$. $p_{E|canny}$ and $p_{E|OSTU,canny}$ stand for the pixel in edges obtained from our method and the OSTU method, respectively. After working out S_R and S_E, we define the state space S as:

$$S = S_R \times S_E \tag{6}$$

4.2. Defining the Action

We define the action as an increase or a decrease based on current values with a specific step size T. Therefore, the agent have 9 actions to select in each iteration, which are {[-T,-T], [-T,0], [-T,+T], [0,T], [0,0], [0,+T], [+T,-T], [+T,0], [+T,+T]}. The abundance of the actions ensures that the agent is capable to explore all possible conditions and the state is updated with the action whose corresponding value in Q table is the largest being taken.

4.3. Defining the Reward/Punishment

A standard is indispensable to set up to define a reward or a punishment. Since we have best artificial segmentation versions for each image, we can use them as a criterion to tell how the performance of current segmentation is. A straightforward method is to calculate the coincidence rate between current result and the corresponding best artificial result of an image. If the coincidence rate is low, which means that values of center point pair should be adjusted, we give a negative value to the state as a punishment; on the contrary, we provide state with a positive value as reward. In this paper, we set 0.9 as a threshold. When the coincidence rate is above 0.9, we give a positive reward. Otherwise, we give a negative penalty. Concretely, we have following definitions:

$$C = \frac{\sum p_f \cap \sum p_{f|opt} + \sum p_b \cap \sum p_{b|opt}}{\sum p_f + \sum p_b} \tag{7}$$

$$R = \begin{cases} 10*C & C \geq 0.9 \\ -1 & C < 0.9 \end{cases} \tag{8}$$

Where $p_{f|opt}$ and $p_{b|opt}$ are the foreground and background pixels of the optimal segmentation version, respectively.

5. Experiment Result

5.1. Image Segmentation

After preprocessing, the ROI image is further divided into two sub-images. One sub-image includes the test line and the other includes the control line. The training set consists of 8 sub-images containing test line with different concentration of hCG, where each image has been normalized to a size of 115*270. Then, state space coefficients K_R and K_E are both set to 30, which means for each ROI image there are 900 states in total. To explore/exploit the state space, ε-greedy policy has been employed where the learning rate α and discount rate γ are set to 0.3 and 0.9 respectively.

Action is defined as increasing or decreasing a certain value T for current center point. It is worth mentioning that the value of T should be selected reasonably, either a too large T or a too small T will affect the convergence speed of the RL algorithm. Moreover, learning rate of the RL algorithm also makes a difference in terms of the convergence speed. Based on this verified phenomenon, we implement a test in order to determine the best values of the parameters above, the results are shown in Figure 5. From Figure 5, the algorithm converges with the fewest times of iteration when T=5, α=0.3. Thus we finally choose a step size of 5 and a learning rate of 0.3 in our experiments.

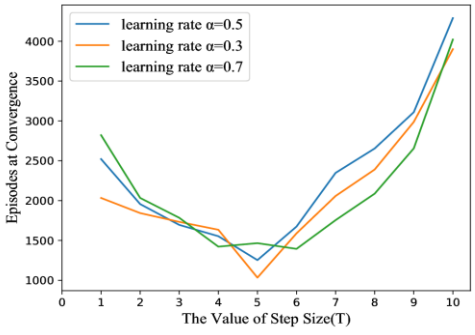

Figure 5. Convergence curves of different step sizes and learning rates.

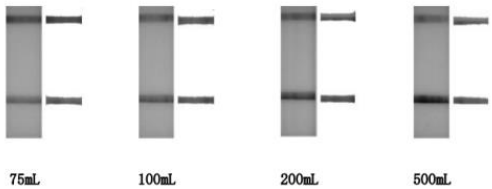

Figure 6. Experimental results of GICS images.

When the training is completed, we use the sub-images with the control lines as the test set. Similarly, each test image also has an artificial best segmentation version that could offer a comparison. To quantitatively evaluate the segmentation results, a similarity measure indicator η has been used to signify the accuracy, which is a general criterion and defined as:

$$\eta = \frac{B_s \cap B_r + F_s \cap F_r}{B_s + F_s} \times 100\% \tag{9}$$

Where the subscript index *r* represents the standard artificial image while *s* is for the segmentation result; the letter *B* and *F* stands for the background and foreground area, respectively. In Figure 6, complete segmentation results are presented, and corresponding accuracies have been listed in Table 1.

Table 1. The classification accuracy of all GICS images.

Concentration	Accuracy of control line (%)	Accuracy of test line (%)	Total accuracy (%)
75mL	93.1	94.0	93.6
100mL	94.9	94.0	94.5
200mL	95.6	94.1	94.9
300mL	95.7	94.4	95.1
400mL	94.2	96.1	95.2
500mL	95.6	94.6	95.1
Average	94.9	94.5	94.7

5.2. Quantitative Analysis

In this part, we propose a quantitative detection method based on the segmented GICS images. For the purpose of characterizing the concentration of hCG in the images, a parameter named relative integrated optical density (RIOD) is introduced in our work [12]. According to Lambert Beer's law, the RIOD value of a GICS image can be calculated as:

$$RIOD = \frac{IOD_T}{IOD_C} = \frac{\sum_{i=1}^{M} \log \frac{G_{avg}}{G_i}}{\sum_{j=1}^{N} \log \frac{G_{avg}}{G_j}} \tag{10}$$

Where IOD_T and IOD_C denote the reflective integral optical density of the test line and control line, respectively. *avg* is the average grayscale of pixels in the whole image, G_j represents the grayscale of pixels in the control line, and G_i represents the grayscale of pixels in the test line, *N* and *M* denote the number of pixels in the test line and the control line respectively. On the basis of formula 10, we calculate the RIOD values of different test samples and the results are shown in Table 2.

Table 2. The RIOD values of different test samples.

Concentration (mL)	75	100	150	200	300	400	500
RIOD	0.6523	0.9481	1.0572	1.6493	1.9936	2.7429	3.7415

As can be seen from Table 2, the higher the concentration is, the larger the RIOD value will be, which means that there is a linear relationship between the two quantities. Therefore, a functional relationship can be obtained through the least square method. Once the function is confirmed, the hCG concentration of a new image can be predicted as long as we know its RIOD value.

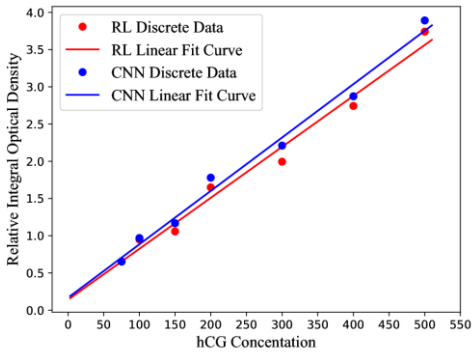

Figure 7. Linear fit schematic.

According to the data in Table 2, we make the scatter plot and the least squares fitting as shown in Figure 7. The correlation coefficient of the fitted line is 0.9631, which indicates the concentration of hCG and the RIOD value are highly linearly dependent. For comparison, Figure 7 also show the straight line fitted of the segmentation image using the adaptive cellular neural network (CNN). While the correlation coefficient of CNN segmentation result is 9.5969. As a result, the goal of quantitative detection can be achieved by means of calculating the RIOD value of a new segmented image.

6. Conclusion

In this paper, we applied reinforcement learning to construct a novel quantitative analysis model of gold immunochromatographic strips to achieve accurate segmentation of GICS images. We perform experiments on hCG images in different levels of concentration and the results demonstrate that our model exhibits satisfactory performance regardless the concentration. Furthermore, we quantitatively analyze the segmentation results of GICS images and find that there is a good linear relationship between their RIOD and concentration, which shows that the goal of quantitative analysis can be achieved. Future work should make full use of reinforcement learning, which has been used in various research fields due to its high adaptability and strong vitality, especially in image processing and intelligent control [13]. Enhancing the performance of the reinforcement model is a promising work and we can optimize the state space to develop a more advanced image segmentation method.

References

[1] Yager, P., Edwards, T., Fu, E., Helton, K., Nelson, K., Tam, M. R. (2006) Microfluidic diagnostic technologies for global public health, Nature., 442: 412-418.
[2] Qian, S., Haim, H. (2003) A mathematical model of lateral flow bioreactions applied to sandwich assays, Anal Biochem., 322: 89–98.
[3] Kaur, J., Singh, K., Boro, R., Thampi, K., Raje, M., Varshney, G. (2007) Immunochromatographic dipstick assay format using gold nanoparticles labeled protein-hapten conjugate for the detection of atrazine, Environ Sci Technol., 41: 5028-5036.
[4] Zeng, N., Wang, Z., Li, Y., Du, M., Cao, J. Liu, X. (2013) Time series modeling of nano-gold immunochromatographic assay via expectation maximization algorithm, IEEE Trans Biomed Eng., 60: 3418-3424.
[5] Zeng, N., Wang, Z., Zineddin, B., Li, Y., Du, M. (2014) Image-based quantitative analysis of gold immunochromatographic strip via cellular neural network approach, IEEE Trans Med Imaging., 33: 1129-1136.
[6] Zeng, N., Wang, Z., Zhang, H. and Alsaadi, F. E. (2016) A novel switching delayed PSO algorithm for estimating unknown parameters of lateral flow immunoassay, Cognitive Computation., 8: 143-152.

[7] Kiumarsi, B., Vamvoudakis, K. G., Modares, H., Lewis, F. L. (2018) Optimal and Autonomous Control Using Reinforcement Learning: A Survey, IEEE Transactions on Neural Networks and Learning Systems., 29: 2042-2062.
[8] Sutton, R. S., Barto, A. G. (2018) Reinforcement Learning: An Introduction., MIT Press, Cambridge.
[9] Watkins, C.J.C.H., Dayan, P. (1992) Q-Learning, Machine Learning., 8: 279-292.
[10] Yan, J., He, H., Zhong, X., Tang, Y. (2017) Q-Learning-Based Vulnerability Analysis of Smart Grid Against Sequential Topology Attacks. IEEE Transactions on Information Forensics and Security., 12: 200-210.
[11] Wang. Z.Y., Shi, Z.G., Liu, Y.K,, Tian. J. (2013) The optimization of path planning for multi-robot system using Boltzmann Policy based Q-learning algorithm., IEEE ., 36: 1199 - 1204.
[12] Zeng, N., Wang, Z., Zhang, H., Liu, W., Alsaadi, F. E. (2016) Deep belief networks for quantitative analysis of gold immunochromatographic strip, Cognitive Computation., 8: 684-692.
[13] Zeng, N., Zhang, H., Song, B., Liu, W., Li, Y., Dobaie, A. M. (2018) Facial expression recognition via learning deep sparse autoencoders, Neurocomputing., 273: 643-649.